XRD and TEM study of high-pressure treated single-walled carbon nanotubes and C_{60}-peapods

S. Kawasaki *,

Department of Materials Science and Engineering, Graduate School of Engineering, Nagoya Institute of Technology, Gokiso-cho, Showa-ku, Nagoya 466-8555, Japan

Y. Matsuoka, T. Yokomae, Y. Nojima, F. Okino, H. Touhara

Faculty of Textile Science and Technology, Shinshu University, 3-15-1 Tokida, Ueda 386-8567, Japan

H. Kataura

Nanotechnology Research Institute, National Institute of Advanced Industrial Science and Technology (AIST) Central 4, Higashi 1-1-1, Tsukuba, Ibaraki 305-8562, Japan

---

Abstract

In situ synchrotron X-ray diffraction measurements of single-walled carbon nanotube and C_{60}-peapod samples under high pressures up to 13 GPa and at high temperature were carried out. Anisotropical shrinkages of their bundle 2-dimensional lattices by compression at room temperature were observed. It was found that the lattices recover original forms reversibly upon pressure release. It was also found

that irreversible phase transformations occur by raising temperature at the highest pressure. The high-pressure and high-temperature treated samples were examined by X-ray diffraction, transmission electron microscope, and Raman measurements. It was indicated by transmission electron microscope observation that hexagonal diamond is able to be synthesized by high pressure and high temperature treatment of C_{60}-peapods.

Key words: A. Carbon nanotubes; A. Fullerene; C. X-ray diffraction

1 Introduction

Both fullerenes (e.g. C_{60}, C_{70}) and carbon nanotubes are fascinating materials, not only because they have unique structures, but also because they exhibit extraordinary physical properties. Since they are constructed from sp^2 carbons having strong atomic bonds, these molecules themselves show very high stiffness. It is well known that the bulk modulus of C_{60} molecule is calculated to be 843 GPa [1], which is much greater than that of diamond (441 GPa), and that many theoretical studies of single-walled carbon nanotubes (SWNTs) give the value of axial Young's modulus in Tera Pa range [2]. However, their bulk crystals behave as soft materials, because the bulk crystals consist of such hard molecules bound by weak van der Waals interaction.

The capability of carbon to form sp^3 bonding between fullerene molecules provides a possibility for the creation of superhard carbon nanocluster-based materials. In fact, high-pressure and high-temperature (HPHT) treatments of

* fax:+81-52-735-5221
Email address: kawasaki.shinji@nitech.ac.jp (S. Kawasaki).

solid C_{60} produce a variety of phases of polymerized C_{60} known as "fullerene polymers" [3]. So far, three crystalline phases and some amorphous phases of polymerized fullerenes were synthesized. One of the amorphous phases have hardness high enough to scratch the (111) face of diamond [4–7].

High pressure behaviors of carbon nanotubes have also been investigated by X-ray diffraction (XRD), Raman scattering and so on [8–17]. There are many reports on high pressure behavior of SWNTs using a diamond anvil cell (DAC) at room temperature, while only a few HPHT experiments of SWNT sample were reported. Khabashesku et al. [15] have done transmission electron microscope (TEM) observation and Raman scattering, XRD measurements of the SWNT samples HPHT treated up to 9.5 GPa, 1873 K and discussed the possibility of polymerization of SWNTs. Unfortunately, since the SWNT sample used in their experiment was not well crystallized and did not exhibit any diffraction peaks, it is difficult to discuss the structural change of bundle crystal by HPHT treatment. In the present study, we have performed in situ XRD experiment of well crystallized SWNT sample under pressures higher than 10 GPa and at high temperatures. TEM observation and Raman scattering measurements of the HPHT treated SWNT samples were also carried out in order to clarify the structural change.

C_{60}-peapod, a SWNT including C_{60} molecules inside the tube, is one of the new nanocarbon materials and is attracting much interest regarding physical properties, especially in elastic property. Therefore, we have performed the above mentioned experiments not only for SWNT samples but also for C_{60}-peapod samples.

2 Experimental

2.1 Sample preparation

The SWNT samples used in the present study were prepared by laser-ablation method. The detailed procedures of synthesis and purification are written elsewhere [18]. The tube diameter is estimated to be 1.4-1.5 nm by Raman scattering measurement of radial breathing modes (RBM). For the preparation of C_{60}-peapod sample, after decapping the SWNTs, C_{60} was introduced into tubes by heating C_{60} powders with SWNTs in a sealed quartz tube. The C_{60}-occupancy of the pods was estimated to be more than 80% by TEM observation.

The angular-dispersive (AD) XRD patterns of the SWNT and C_{60}-peapod samples in the form of foils called buckypaper were measured by a conventional powder diffractometer with a SiO_2 reflection-free sample plate.

2.2 In situ XRD measurements

In situ energy-dispersive (ED) XRD measurements under high pressure were performed with a cubic anvil press (MAX80) at a beam line AR-NE5C of High Energy Accelerator Research Organization (KEK), Tsukuba, Japan. A synchrotron white X-ray at AR-NE5C of KEK was used as an incident beam and a diffracted beam was measured with a pure Ge solid state detector. A BN capsule in which a SWNT (or C_{60}-peapod) sample was charged with NaCl was inserted into the center of a $(6\ \mathrm{mm})^3$ cubic pressure-transmitting medium consisting of a mixture of amorphous boron and epoxy resin (Fig. 1 (a)). In

order to get random orientation of the sample, the SWNT (or C_{60}-peapod) sample having a foil form was rolled up to a sphere like a bead and some sample beads were crammed into a BN capsule. A pair of graphite disk furnaces were also installed in the pressure cell. Generated pressure was determined from the unit cell parameter of NaCl with Decker's equation of state [19]. The diffraction angles were set at 2θ=3°.

The experimental procedure was as follows. Firstly, the sample was compressed up to about 13 GPa or 11 GPa at room temperature for SWNT or C_{60}-peapod samples, respectively and then, at the highest pressure, heated up to a specific temperature for about 1 h. Thereafter, the sample was quenched down to room temperature under pressure and subsequently the pressure was released.

2.3 Characterization of HPHT treated samples

TEM observation of the HPHT treated samples were done on a JEOL-JEM2010 working at 200 keV. For TEM observation, a part of the HPHT treated sample, obtained as a pellet, was chunked using a razor blade on a glass plate and crushed with an agate mortar, and was dispersed ultrasonically into a alcohol bath. Then, the dispersed sample was transferred to a TEM grid. Another part of the pellet of the HPHT treated sample was used for Raman scattering measurement on a JASCO NRS-2100F. The excitation source was a 514.5 nm Ar laser line. The laser power was tuned at 70 mW.

3 Results & Discussion

Fig. 2 shows the angular-dispersive XRD patterns of the SWNT and C_{60}-peapod samples under atmospheric pressure and at room temperature. As shown in Fig. 2, it was found that the samples were well crystallized. Since the contribution of the structure factor of C_{60} chain inside the tube reduces the total structure factor at the 10 peak position [18], the 10 peak intensity of the C_{60}-peapod sample is much lower than that of the SWNT sample, confirming that C_{60} molecules were filled in the tubes of the C_{60}-peapod sample.

The change in XRD pattern of the SWNT sample with increasing pressure at room temperature is shown in Fig. 3. As shown in Fig. 3, the diffraction pattern were clearly observed for the sample in a pressure cell at ambient pressure. Comparing the pattern with Fig. 2 (a), the relative intensity of 10 peak is found to be smaller, because the effective X-ray photon flux in low energy regions is reduced more easily by the absorption in the beam path. It was observed that the shifts of the diffraction peak positions greatly vary with *hkl* indicies (Fig. 4). At the highest pressure, the samples were heat-treated but no remarkable change in XRD pattern was observed during the heat-treatment. Fig. 5 shows the change in XRD pattern with decreasing pressure at room temperature after HPHT treatments at about 13 GPa and at RT, 473 K, and 873 K (for convenience, these samples were abbreviated as SWNT-RT, SWNT-473 and SWNT-873, respectively). As shown in Fig. 5 (a), SWNT-RT recovered the initial diffraction pattern on pressure release except that the 10 peak intensity became smaller comparing with the initial intensity. The reduction of the 10 peak intensity is considered to be due to the increase of absorption of low energy X-ray in the beam path which is caused

by the deformation of boron-epoxy resin pressure-transmitting medium (Fig. 1 (c)). SWNT-473 also recovered the initial pattern at 0.1 MPa although the lowering of the crystallinity was observed. Therefore, in these two samples, no irreversible transformation occurred. On the other hand, since the observed diffraction pattern of SWNT-873 on complete release of pressure is different from the initial pattern, an irreversible phase transformation might have occurred by the treatment. The lowest energy peak (denoted by 10^{d} in Fig. 4 (c)) of the transformed phase shows a flat compression curve. It indicates that the transformed phase is much harder than the pristine phase.

This transformation was also confirmed by Raman scattering experiments of the HPHT treated samples. Since tangential mode (G-band) at about 1590 cm^{-1} and RBM mode were clearly observed in the spectra (Figs. 6 (b), (c)) of SWNT-RT and SWNT-473, the tubes of these samples were mostly maintained. However, it was also found that the tube structures of these two samples were damaged by HPHT treatments, because the relative intensity of the disordered band (D-band) at about 1350 cm^{-1} to G-band increased compared with that of pristine sample in both two cases. On the other hand, no sharp peak is seen in the spectrum of SWNT-873 (Fig. 6 (d)). It indicates that the transformation was caused by the significant deformations of the tubes.

In order to investigate the local structures of the HPHT treated SWNT samples, TEM observation was carried out. In the cases of SWNT-RT and SWNT-473 samples, bundles of SWNTs were observed as in the case of pristine SWNT sample (Figs. 7 (a-1), (a-2)). The selected area electron diffraction (SAD) patterns of SWNT-RT and SWNT-473 samples also resemble that of the pristine sample (Figs. 7 (b-1), (b-2)). Fig. 7 (b-1) shows a typical example of SAD pattern of SWNT bundles. Several diffraction spots caused by the bundle

2D triangular lattice in the central line and two concentric diffraction rings defined by a transfer momentum k_1 ($k_1 = 2\pi/d_1$ with $d_1 = 3d_{C-C}/2$ and $d_{C-C} = 0.142$ nm is the carbon-carbon distance) and a k_2 ($k_2 = 2\pi/d_2$ with $d_2 = \sqrt{3}d_{C-C}/2$) [20] are seen in Figs. 7 (b-1) and 7 (b-2). On the other hand, no tube structure could be found in SWNT-873 and structureless materials as shown in Fig. 7 (a-3) were often observed. No diffraction pattern was detected in most part of SWNT-873 sample. Occasionally, however, very weak diffraction rings having $d = 0.34$ nm and $d = 0.17$ nm which indicate the existence of graphite-like atomic arrangement were observed (Fig. 7 (b-3)).

Fig. 8 shows the change in ED XRD pattern of C_{60}-peapod sample with increasing pressure at room temperature. In the present experiment, unfortunately, 10 peak of C_{60}-peapod was not observed even at atmospheric pressure, probably due to the low scattering factor of C_{60}-peapod at the 10 peak position and the small photon flux in low X-ray energy regions. A diffraction peak at 25.23 keV (marked "C_{60}" in Fig. 8), corresponding to $d = 0.956$ nm ($2\theta = 2.946°$), is due to the reflection from 1D C_{60} crystals inside the SWNTs. The "C_{60}" diffraction peak is not seen in the AD XRD pattern (Fig. 2 (b)), probably because highly oriented SWNTs in buckypaper on a SiO_2 plate may inhibit the satisfaction of diffraction condition. It was found that the "C_{60}" peak intensity increase by compression (Fig. 8). The reason is not clear but can be explained as follows. At ambient pressure, C_{60} molecules were packed loosely and the crystallinity of the 1D C_{60} crystal was not so high. However, C_{60} molecules might be aligned well on compression and the crystallinity became better. C_{60}-C_{60} cluster distance decreases from 0.956 nm at 0.1 MPa down to 0.892 nm at 10.7 GPa (Fig. 9) which is much smaller than the nearest C_{60}-C_{60} distance in a rhombohedral C_{60} polymer. On the other hand, the

bundle 2D lattice of C_{60}-peapod sample also deforms by compression as that of the SWNT sample does. The pressure shift of 21 diffraction line of the C_{60}-peapod sample is determined to be 2.01×10^{-3} nm/GPa and the value is almost the same as that of the SWNT sample. Therefore, the bulk crystal of C_{60}-peapod sample does not become to be much harder than that of SWNT sample, although C_{60}-peapod sample includes C_{60} molecules which are considered to be very hard.

In the present experiment, unfortunately, the diffraction intensity became very weak abruptly above 11 GPa probably due to bad alignments of the anvils. Then we gave up further compression and raised temperature at the pressure. Therefore, we could not observe the diffraction pattern during temperature rise and pressure release. Fig. 10 shows the AD XRD patterns of C_{60}-peapod samples which were HPHT treated at 11 GPa, and at RT and 873 K, (these samples are abbreviated as Peapod-RT and Peapod-873, respectively), at ambient pressure and at RT. As shown in Fig. 10, Peapod-RT recovered the initial diffraction pattern, while only a broad peak at about 22° is seen in the pattern of Peapod-873. Therefore, it is considered that the bundle triangular lattice of Peapod-873 deteriorated by the HT treatment. Fig. 11 shows the observed Raman spectra of Peapod-RT and Peapod-873. The Raman spectrum of Peapod-RT is almost the same as that of pristine C_{60}-peapod sample except that the G-band peak profile is a little broader. On the other hand, the reduction in intensity and broadening of the G-band Raman peak and the increase of the D-band peak are seen in the spectrum of Peapod-873 (Fig. 11 (c)). However, since RBM peak was observed in Fig. 11 (c) although its intensity was much reduced, not all the tubes were collapsed. This was also confirmed by TEM observation. As shown in Fig. 12, it is hard to find tube structures

in TEM images of Peapod-873. However, two diffraction rings related to the momenta k_1 and k_2, indicating the existence of the tube, were observed in a SAD pattern of some domains of Peapod-873. It should be noted that the central line due to the bundle 2D lattice was no longer detected in the SAD pattern. This is consistent with AD XRD experimental result. Judging from these results, it is considered that the bundle 2D lattice is broken down by HPHT treatment while the tube structure does not collapse completely.

We observed an another interesting SAD pattern shown in Fig. 12 (b-3) from Peapod-873. This pattern could be indexed as an a^*b^* plane of hexagonal diamond (lonsdaleite) which is usually synthesized by dynamical high pressure treatment. It is very interesting if hexagonal diamond can be synthesized by a static high pressure treatment of C_{60}-peapod and it is very useful so as to consider the formation mechanism of the hexagonal diamond.

4 Conclusion

In situ synchrotron XRD measurements of SWNT and C_{60}-peapod samples under high pressure were performed. Several diffraction lines of these two samples were able to be observed under high pressure. The followings were found.

(1) The 2D bundle lattices of these two samples shrink anisotropically by compression.

(2) The pressure shifts of the diffraction lines of these two samples are not different much from each other.

(3) The C_{60}-C_{60} cluster distance in C_{60}-peapods decreases from 0.956 nm at

0.1 MPa down to 0.892 nm at 10.7 GPa.

It was also found that these two samples are transformed irreversibly by raising temperature under high pressure. Interestingly, it was indicated by TEM observation that hexagonal diamond is able to be synthesized by HPHT treatment of C_{60}-peapods.

The phase stabilities of SWNT and C_{60}-peapod pseudo-two-dimensional crystals in a wide pressure-temperature region were elucidated by this work.

Acknowledgement

The authors are grateful to Mr. Narita, Prof. Nagai, Prof. Yamanaka of Osaka University for Raman scattering experiments. This work was supported in part by a Grant-in-Aid for 21st Century COE Program by the Ministry of Education, Culture, Sports, Science and Technology of Japan, and in part by the Kazuchika Okura Memorial Foundation. H.K. acknowledges for a support by Industrial Technology Research Grant Program in '03 from New Energy and Industrial Technology Development Organization (NEDO) of Japan.

References

[1] Ruoff RS, Ruoff AL, Is C60 stiffer than diamond? Nature 1991; 350: 663-664.

[2] Krishnan A, Dujardin E, Ebbesen TW, Yianilos PN, Treacy MMJ, Young's modulus of single-walled nanotubes. Phys. Rev. B 1998; 58: 14013-14019.

[3] Iwasa Y, Arima T, Fleming RM, Siegrist T, Zhou O, Haddon RC, et al. New phases of C60 synthesized at high pressure. Science 1994; 264: 1570-1572.

[4] Blank V, Popov M, Buga S, Davydov V, Denisov VN, Ivlev AN, et al. Is C60 fullerite harder than diamond? Phys. Lett. 1994; 188: 281-286.

[5] Blank VD, Buga SG, Serebryanaya NR, Dubitsky GA, Bagramov RH, Popov MY, et al. Physical properties of superhard and ultrahard fullerites created from solid C60 by high-pressure-high-temperature treatment. Appl. Phys. A 1997; 64: 247-250.

[6] Blank VD, Denisov VN, Lvlev AN, Mavrin BN, Serebryanaya NR, Dubitsky GA, et al. Hard disoredered phases produced at high-pressure-high-temperature treatment of C60. Carbon 1998; 36: 1263-1267.

[7] Blank VD, Buga SG, Serebryanaya NR, Dubitsky GD, Mavrin BN, Popov MY, et al. Structures and phisical properties of superhard and ultrahard 3D polymerized fullerites created from solid C60 by high pressure high temperature treatment. Carbon 1998; 36: 665-670.

[8] Tang J, Qin L, Sasaki T, Yudasaka M, Matsushita A, Iijima S, Compressibility and polygonization of single-walled carbon nanotubes under hydrostatic pressure. Phys. Rev. Lett. 2000; 85: 1887-1889.

[9] Tang J, Qin L, Sasaki T, Yudasaka M, Matsushita A, Iijima S, Compressibility and ploygonization of single-walled carbon nanotubes under hydrostatic pressure. J. Phys.: Condens. Mater. 2002; 14: 10575-10578.

[10] Sharma SM, Karmakr S, Sikka SK, Teredesai PV, Sood AK, Govindaraj A, et al. Pressure-induced phase transformation and structural resilience of single-wall carbon nanotube bundles. Phys. Rev. B 2001; 63: 205417-1-5.

[11] Popov M, Kyotani M, Nemanich RJ, Koga Y, Superhard phase of single wall carbon nanotube: comparison with fullerite C60 and diamond. Phys. Rev. B 2002; 65: 033408-1-4.

[12] Gaál R, Salvetat JP, Forró L, Pressure dependence of the resistivity of single-wall carbon nanotube ropes. Phys. Rev. B 2000; 61: 7320-7323.

[13] Peters MJ, McNeil LE, Lu JP, Kahn D, Structural phase transition in carbon nanotube bundles under pressure. Phys. Rev. B 2000; 61: 5939-5944.

[14] Loa I, Raman spectroscopy on carbon nanotubes at high pressure. J. Raman Spectroscopy 2003; 34: 611-627.

[15] Khabashesku VN, Gu Z, Brinson B, Zimmerman JL, Margrave JL, Davydov VA, et al. Polymerization of single-wall carbon nanotubes under high pressures and high temperatures. J. Phys. Chem. B 2002; 106: 11155-11162.

[16] Rols S, Goncharenko IN, Almairac R, Sauvajol JL, Mirebeau I, Polygonization of single-wall carbon nanotube bundles under high pressure. Phys. Rev. B 2001; 64: 153401-1-4.

[17] Kawasaki S, Matsuoka Y, Yao A, Okino F, Touhara H, High pressure behavior of single-walled carbon nanotubes and polymerized fullerenes. J. Phys. Chem. Solids 2004; 65: 327-332.

[18] Kataura H, Maniwa Y, Abe M, Fujiwara A, Kodama T, Kikuchi K, et al. Optical properties of fullerene and non-fullerene peapods. Appl. Phys. A 2002; 74: 349-354.

[19] Decker DL, Equation of state of sodium choloride. J. Appl. Phys. 1971; 42: 3239-3244.

[20] Henrard L, Loiseau A, Journet C, Bernier P, Study of the symmetry of single-wall nanotubes by electron diffraction. Eur. Phys. J. B 2000; 13: 661-669.

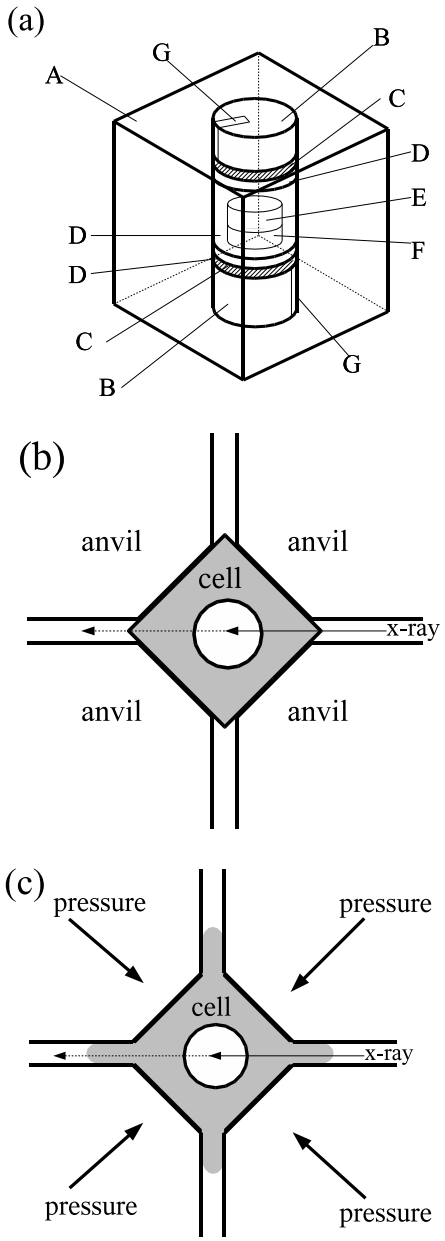

Fig. 1. Schematic pictures of (a) pressure cell assembly, (b) top view of pressure cell and four side anvils before compression, and (c) deformation of the cell by loading pressure (top and bottom anvils are not drawn in (a) and (b)). Notations used in (a); A: boron-epoxy resin, B: pyrophyllite, C: graphite, D: BN, E: NaCl, F: SWNT sample, G: gold foil.

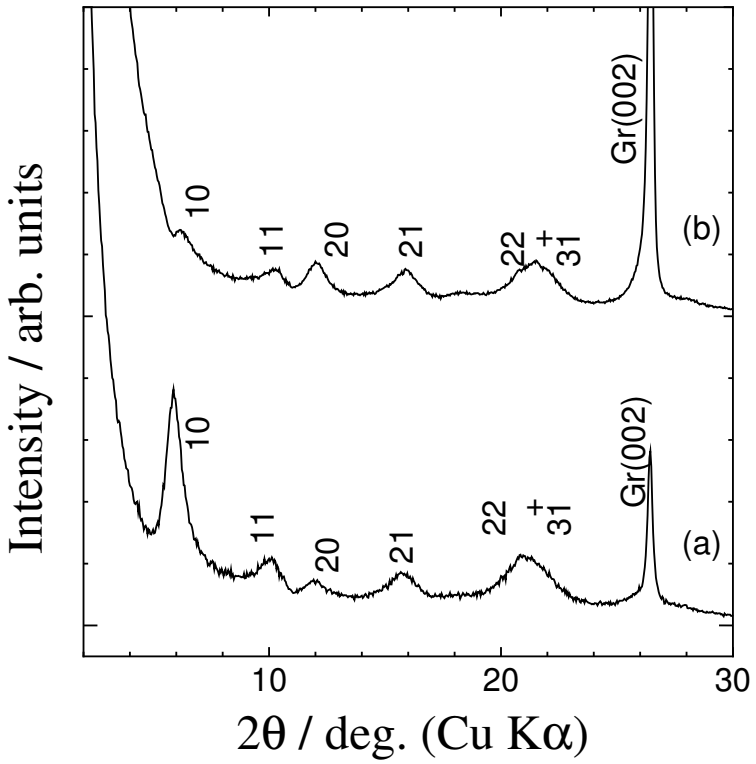

Fig. 2. Angular-dispersive XRD patterns of pristine (a) SWNT and (b) C_{60}-peapod samples. Gr(002) indicates the 002 diffraction peak of graphite impurities.

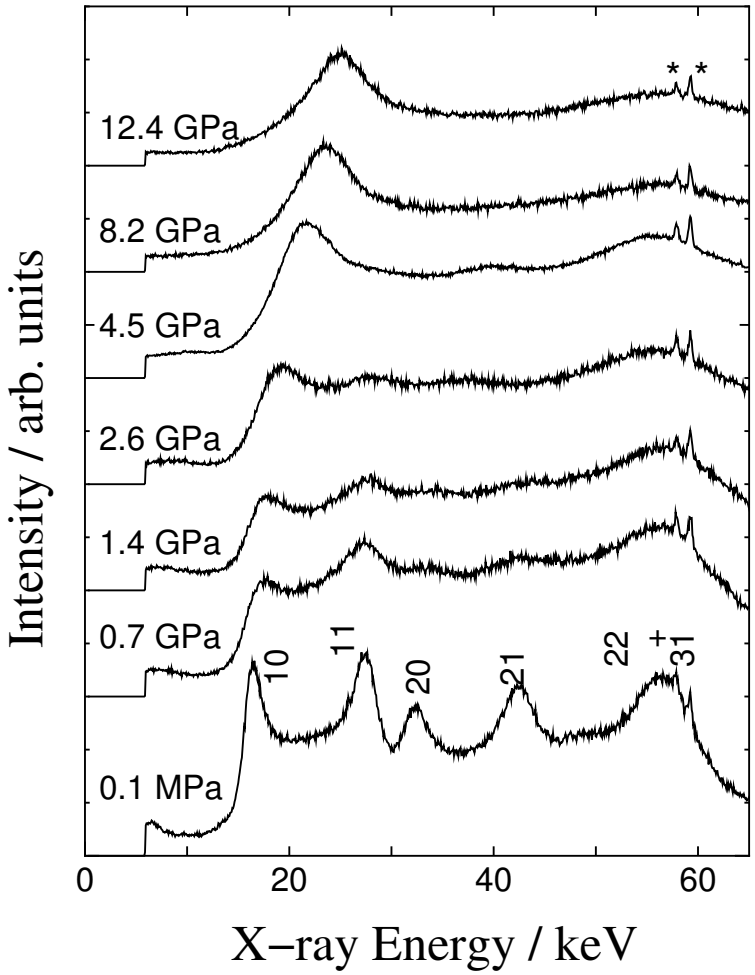

Fig. 3. Change in energy-dispersive XRD pattern of SWNT sample with increasing pressure at room temperature. Asterisks indicate characteristic X-ray peaks of tungsten which was in the beam path.

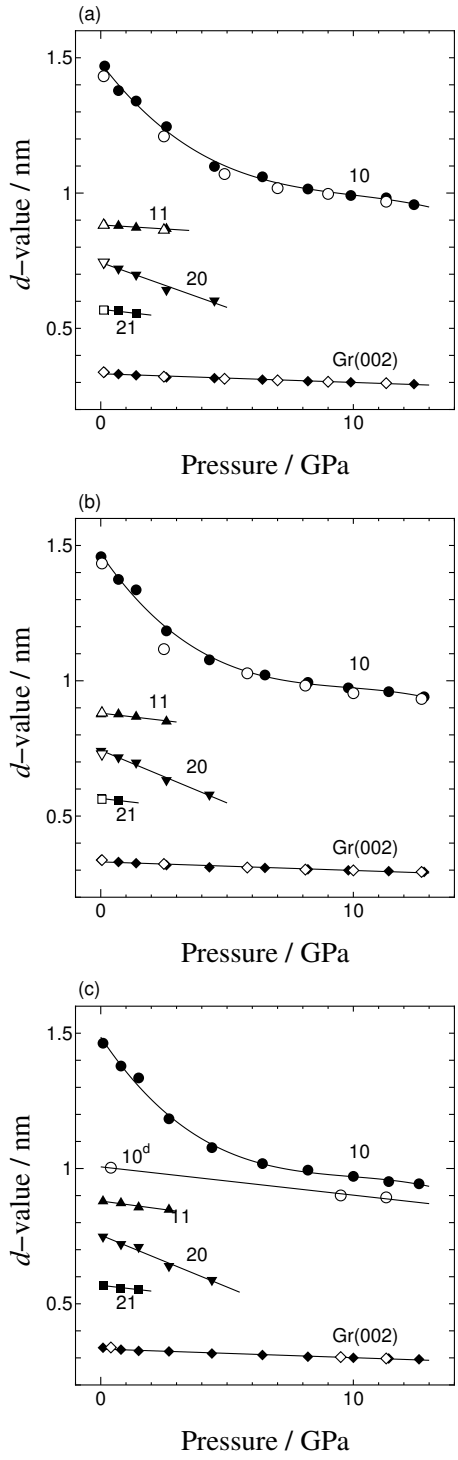

Fig. 4. Pressure dependencies of d-values of (a) SWNT-RT, (b) SWNT-473 and (c) SWNT-873 samples. Filled marks represent data with increasing pressure at room temperature. Open marks represent data with decreasing pressure at room temperature.

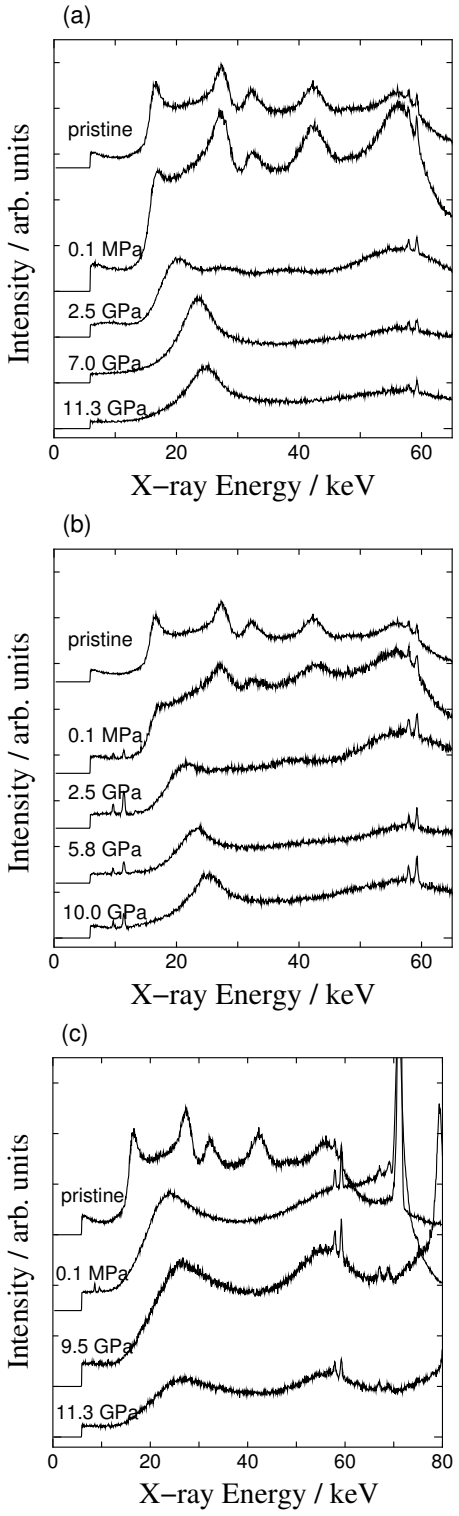

Fig. 5. Change in XRD patterns of (a) SWNT-RT, (b) SWNT-473 and (c) SWNT-873 samples with decreasing pressure at room temperature.

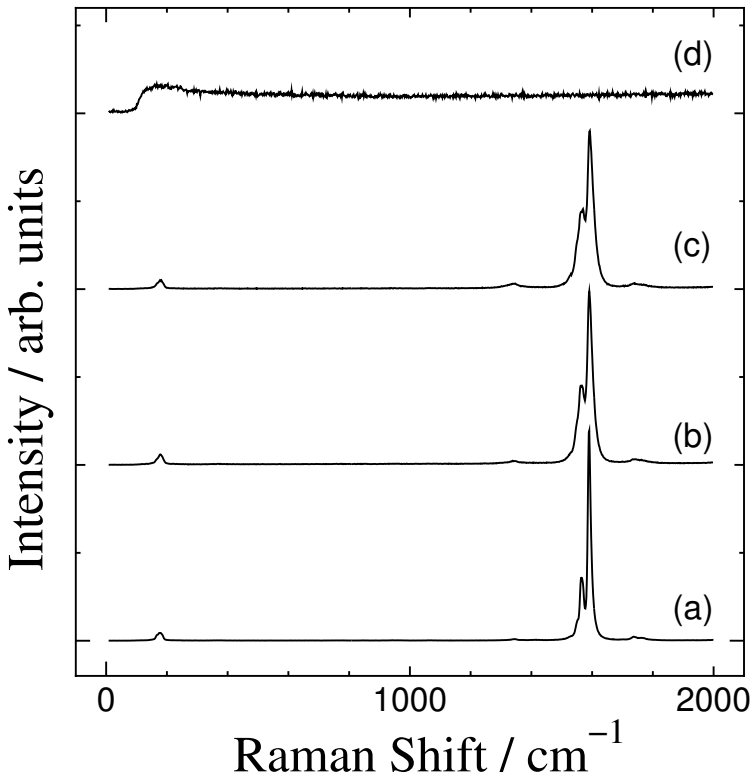

Fig. 6. Raman spectra of (a) pristine SWNT, (b) SWNT-RT, (c) SWNT-473, and (d) SWNT-873 samples.

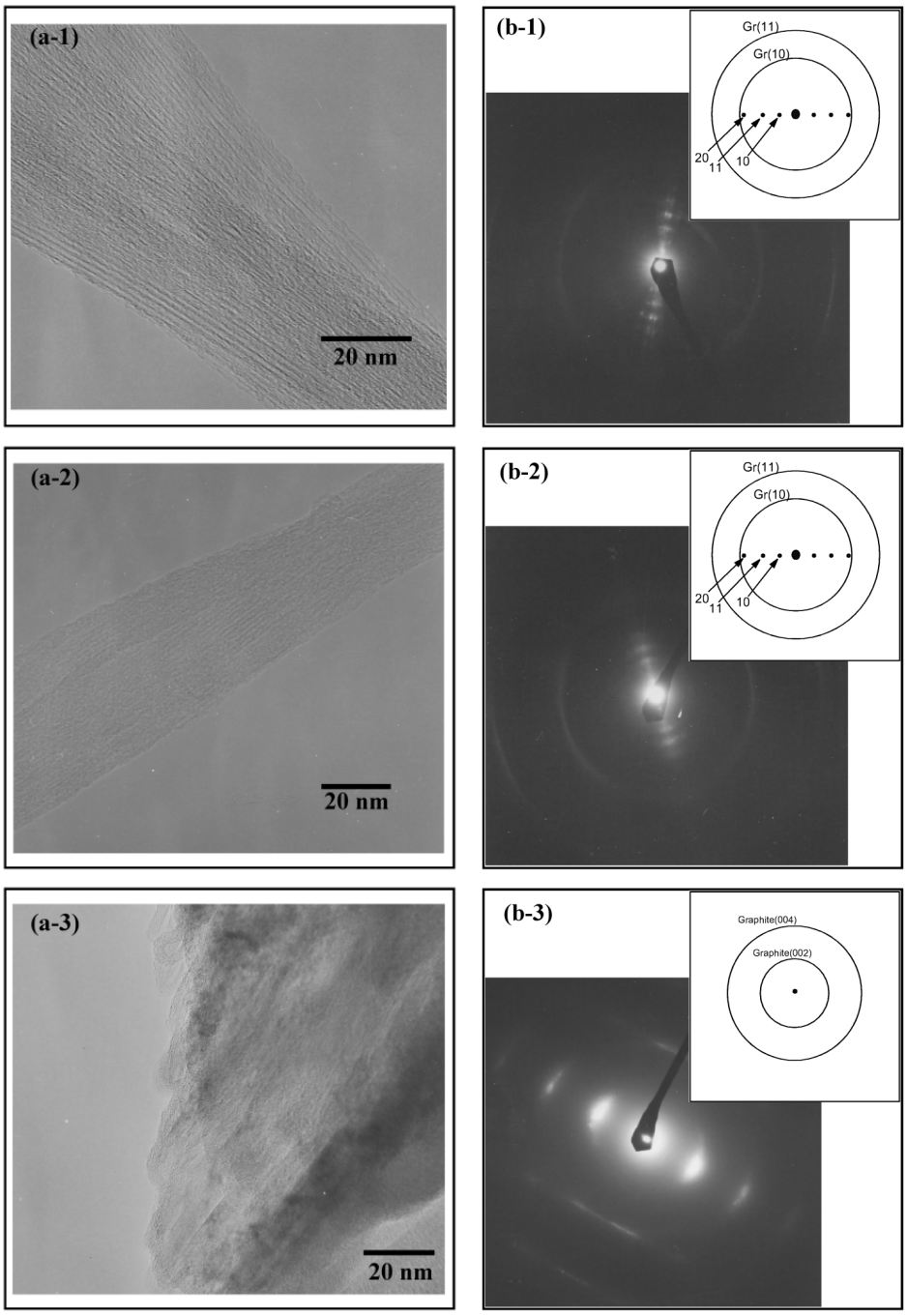

Fig. 7. TEM images of (a-1) pristine SWNT, (a-2) SWNT-473, and (a-3) SWNT-873 samples and corresponding SAD patterns of (b-1) pristine SWNT, (b-2) SWNT-473, and (b-3) SWNT-873 samples.

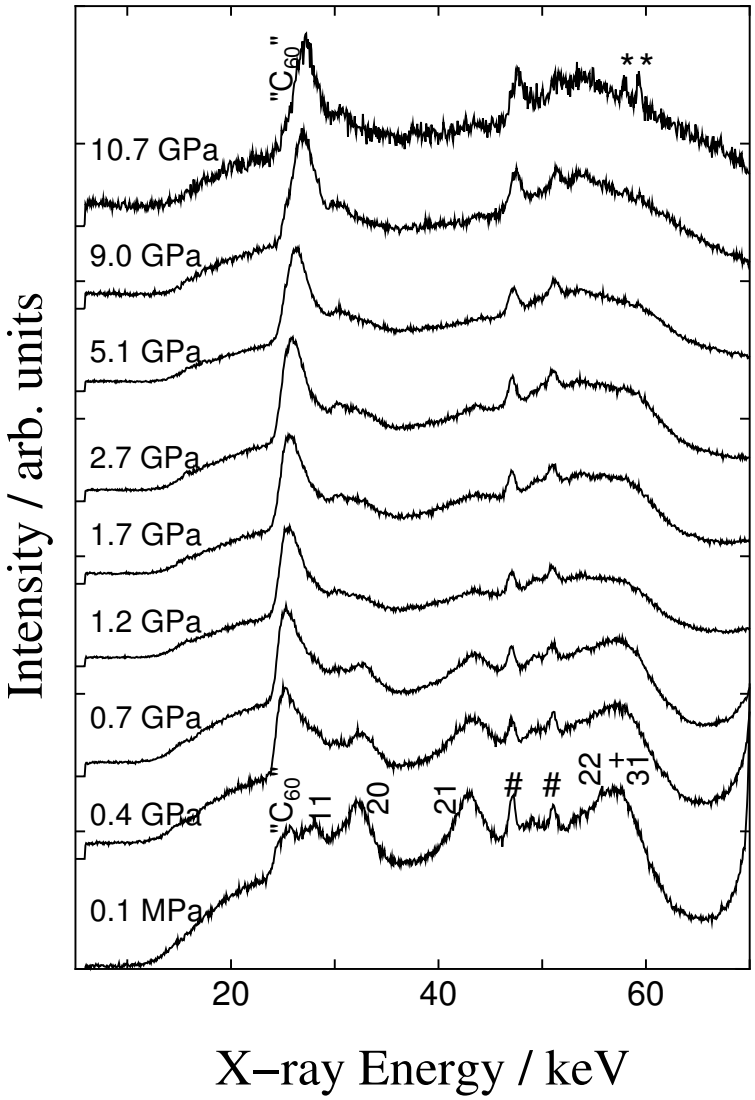

Fig. 8. Change in XRD pattern of C_{60}-peapod sample with increasing pressure at room temperature. Asterisks indicate characteristic X-ray peaks of tungsten which was in the beam path. Sharps (#) denote characteristic X-ray peaks of unknown impurity. "C_{60}" marks denote the diffraction peak of 1D C_{60} crystals inside the SWNTs.

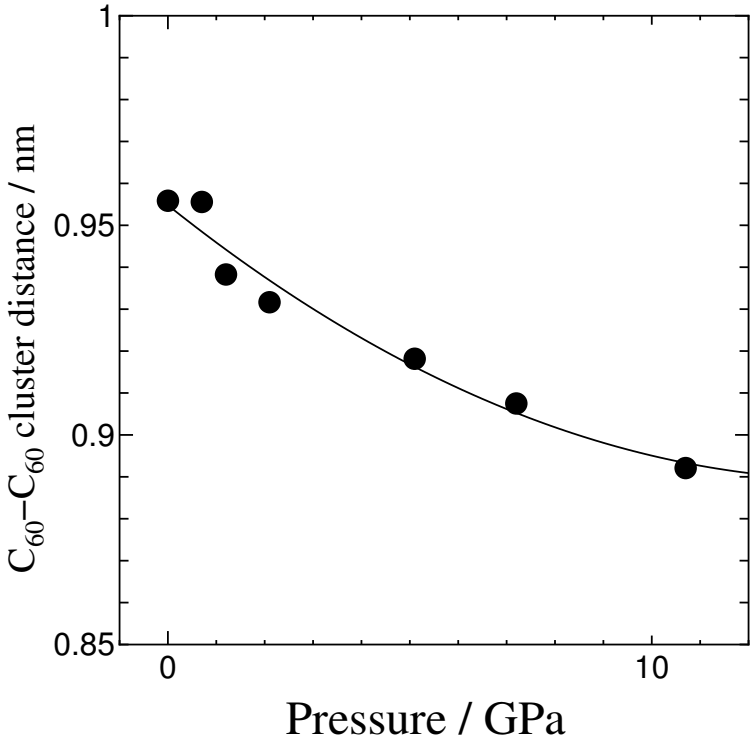

Fig. 9. C_{60}-C_{60} cluster distance in C_{60}-peapod sample as a function of pressure.

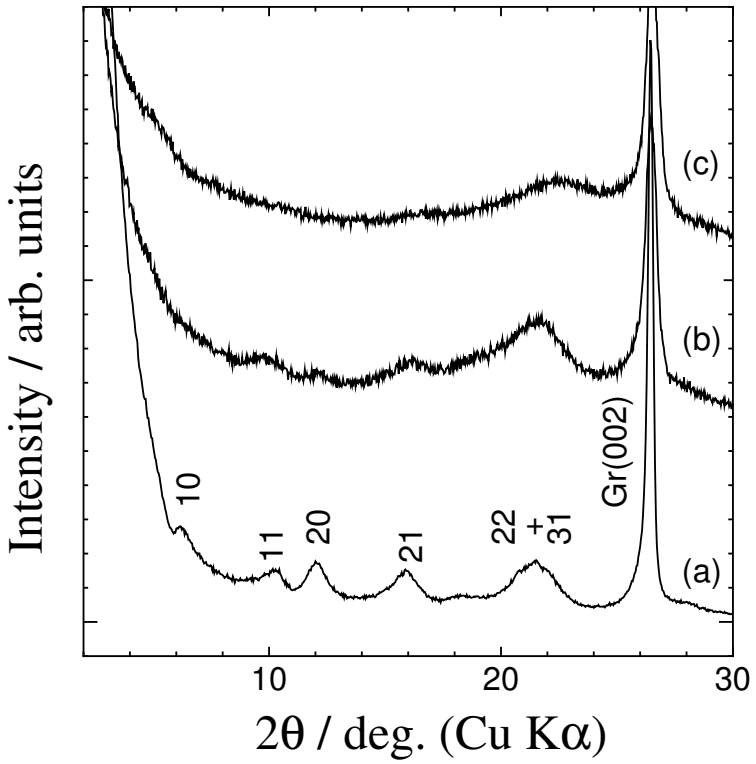

Fig. 10. Angular-dispersive XRD patterns of (a) pristine C_{60}-peapod, (b) Peapod-RT, and (c) Peapod-873 samples. Gr(002) indicates the 002 diffraction peak of graphite impurities.

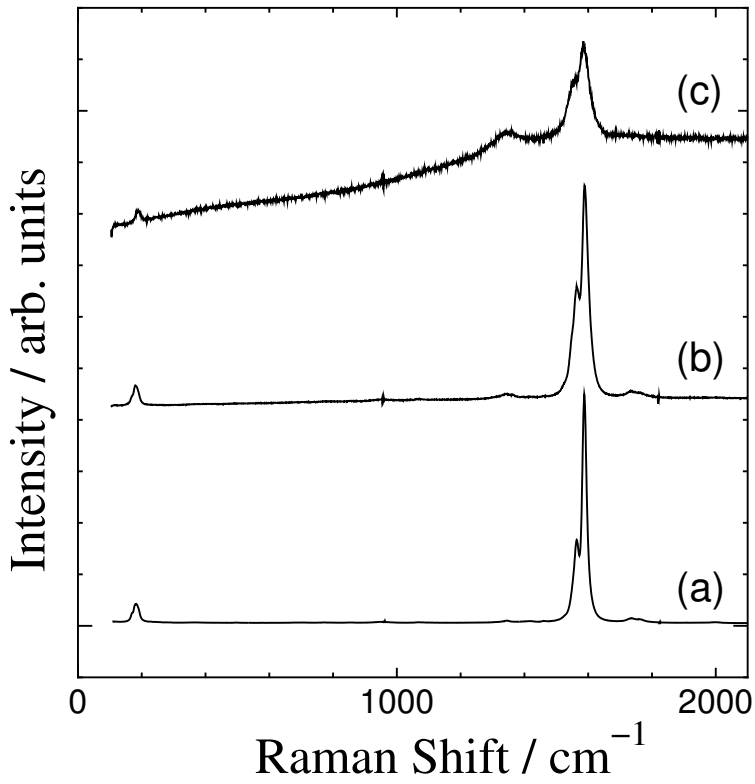

Fig. 11. Raman spectra of (a) pristine C_{60}-peapod, (b) Peapod-RT, and (c) Peapod-873 samples.

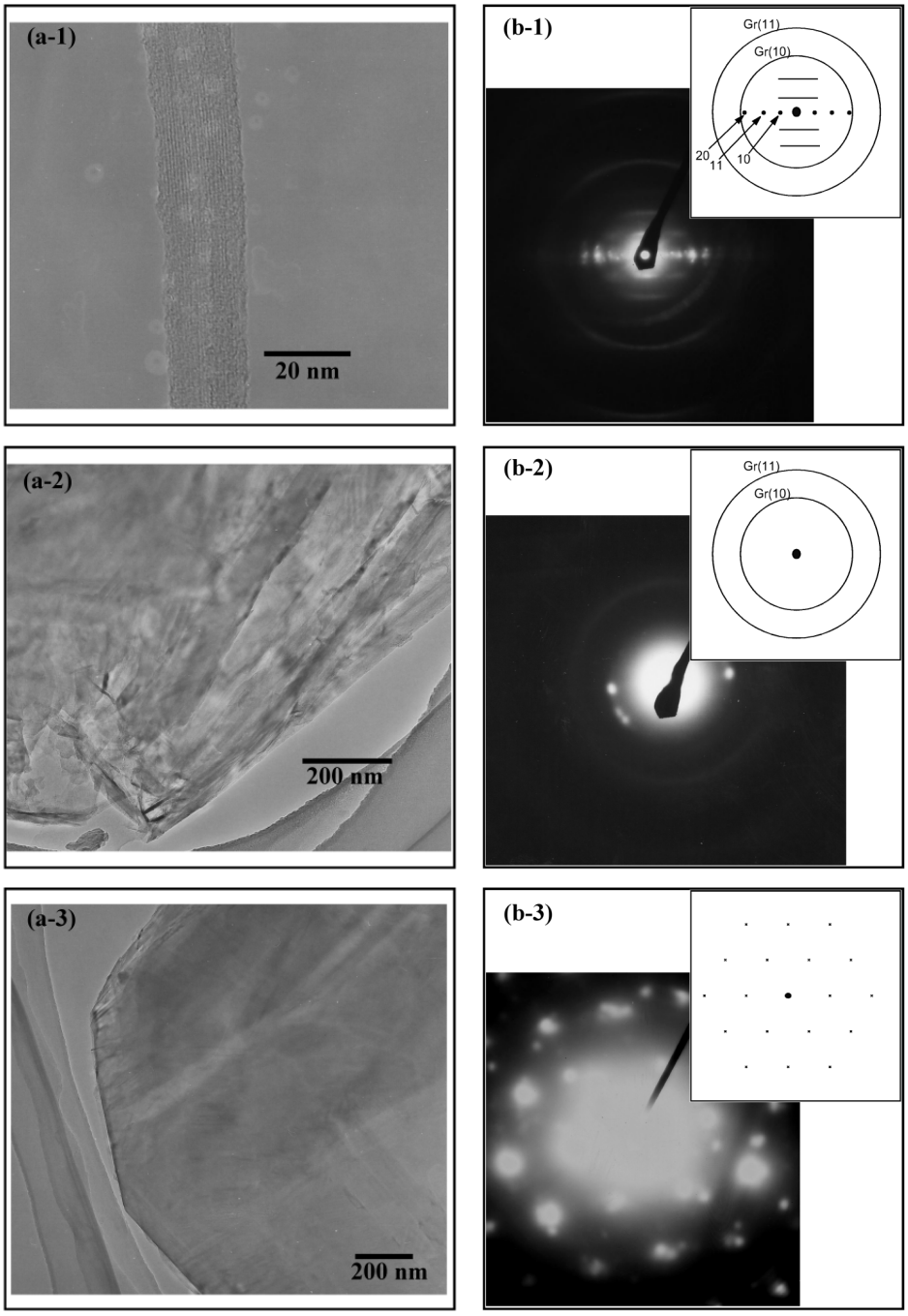

Fig. 12. TEM images of (a-1) pristine C_{60}-peapod and (a-2), (a-3) Peapod-873 samples and corresponding SAD patterns of (b-1) pristine C_{60}-peapod and (b-2), (b-3) Peapod-873 samples.